

Dalton Transactions

Accepted Manuscript



This is an *Accepted Manuscript*, which has been through the Royal Society of Chemistry peer review process and has been accepted for publication.

Accepted Manuscripts are published online shortly after acceptance, before technical editing, formatting and proof reading. Using this free service, authors can make their results available to the community, in citable form, before we publish the edited article. We will replace this *Accepted Manuscript* with the edited and formatted *Advance Article* as soon as it is available.

You can find more information about *Accepted Manuscripts* in the [Information for Authors](#).

Please note that technical editing may introduce minor changes to the text and/or graphics, which may alter content. The journal's standard [Terms & Conditions](#) and the [Ethical guidelines](#) still apply. In no event shall the Royal Society of Chemistry be held responsible for any errors or omissions in this *Accepted Manuscript* or any consequences arising from the use of any information it contains.

ARTICLE

Modulating reactivity in iridium *bis*(N-heterocyclic carbene) complexes: influence of ring size on E-H bond activation chemistry†

Cite this: DOI: 10.1039/x0xx00000x

Received 00th January 2012,
Accepted 00th January 2012

DOI: 10.1039/x0xx00000x

www.rsc.org/

Nicholas Phillips,^a Christina Y. Tang,^a Rémi Tirfoin,^a Michael J. Kelly,^a Amber L. Thompson,^a Matthias J. Gutmann,^b and Simon Aldridge*^a

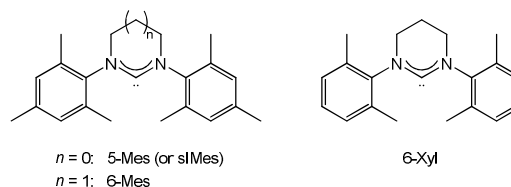
The changes in the steric and electronic properties of N-heterocyclic carbenes (NHCs) as a function of ring size have a profound effect on the reactivity of their late transition metal complexes. Comparison of closely related complexes featuring either a saturated 5- or 6-membered NHC, reveals that the larger ring is associated with an increased propensity towards *intramolecular* C-H activation, but with markedly lower reactivity towards external substrates. Thus, systems of the type $[\text{IrL}_2(\text{H})_2]^+$ give rise to contrasting chemical behaviour, primarily reflecting the differing possibilities for secondary stabilization of the metal centre by the N-bound aryl substituents: highly labile $[\text{Ir}(5\text{-Mes})_2(\text{H})_2]^+$ can only be studied by trapping experiments, while $[\text{Ir}(6\text{-Mes})_2(\text{H})_2]^+$ is air and moisture stable, and unreactive towards many external reagents. With appropriate substrates, this heightened reactivity can be exploited, and *in situ* generated $[\text{Ir}(5\text{-Mes})_2(\text{H})_2]^+$ is capable of intermolecular B-H and N-H activation chemistry. In the case of $\text{H}_3\text{B}\cdot\text{NMe}_2\text{H}$, this affords a rare opportunity to study amine/aminoborane coordination via single crystal neutron diffraction methods.

Introduction

N-heterocyclic carbene (NHC) ligands have in recent years been shown to be effective alternatives to traditional phosphine donors in the stabilization of late transition metal complexes of wide-ranging catalytic relevance.¹ Their strong σ -donor characteristics, for example, offer benefits in terms of metal-ligand bond strength and consequent complex longevity.² In addition, the popular family of ligands based on the unsaturated imidazol-2-ylidene core offers the possibility for wide-ranging and synthetically facile variation in the steric profile of the N-bound substituents. More recently, related 'expanded ring' NHCs, featuring saturated 6- and 7-membered heterocyclic cores have emerged, offering even stronger σ -donor and more sterically demanding ligand profiles.³ The wider NCN angle at the carbenic carbon leads not only to greater carbon 2p character in the HOMO, but is also responsible for the greater demands exerted by the N-substituents in 6-membered NHCs compared to their 5-membered counterparts. Thus, the percentage buried volumes ($\%V_{\text{bur}}$)⁴ calculated for 5-Mes (also known as sIMes) and 6-Mes based on their respective silver(I) halide complexes are 36.1 and 44.0,^{4(0,5)} respectively.

In recent work we have been interested in developing rhodium and iridium complexes featuring ancillary NHC ligands for E-H bond activation processes (E = H, B, C, N).⁶ In particular, we have sought to establish routes to 14-electron

systems of the type $[\text{M}(\text{NHC})_2(\text{H})_2]^+$ and to exploit their reactivity in amineborane dehydrogenation chemistry.^{6(b),(c)} With this in mind, we hypothesized that the size of the supporting heterocyclic ring in saturated NHCs might represent a key variable in controlling the properties of such cations, given the effects that ring size are expected to have on ligand steric/electronic properties. Thus, in the current study we set out to establish synthetic routes to systems of the type $[\text{M}(\text{NHC})_2(\text{H})_2]^+$ featuring the 5-Mes, 6-Mes and (less peripherally bulky) 6-Xyl ligands. A preliminary account of two of these compounds has previously been communicated by us.^{6(h,i)}

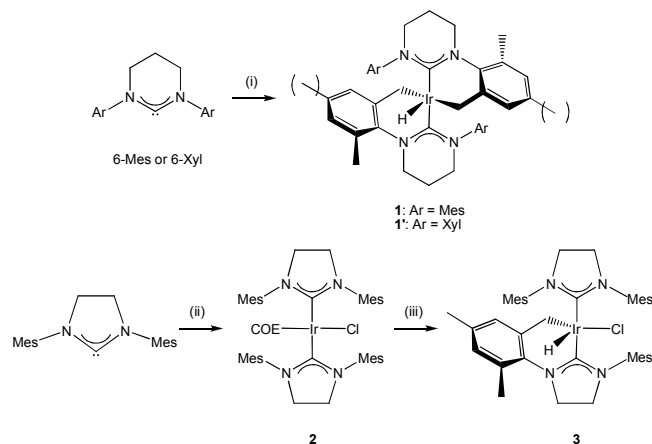


Results and Discussion

Reactions of NHCs with $[\text{Ir}(\text{COE})_2(\mu\text{-Cl})_2]$

The room-temperature reaction of free 6-Mes with dimeric $[\text{Ir}(\text{COE})_2(\mu\text{-Cl})_2]$ in a 6:1 ratio has been shown in preliminary studies to lead to the formation of the doubly C-H activated *bis*(NHC) complex $\text{Ir}(6\text{-Mes}')_2\text{H}$ (**1**; Scheme 1) together with

the hydrochloride salt $[(6\text{-Mes})\text{H}]\text{Cl}$.^{6(h)} While the corresponding chemistry with the related carbene 6-Xyl leads to the formation of the analogous compound $\text{Ir}(6\text{-Xyl})_2\text{H}$ (**1'**), that with 5-Mes proceeds along markedly different lines. Thus, under similar conditions (solvent, temperature, reaction time) no C-H activation is observed, and the planar four-coordinate Ir(I) system $\text{Ir}(5\text{-Mes})_2(\text{COE})\text{Cl}$ (**2**) can be isolated in good yield (see Scheme 1 and Figure 1). More forcing conditions (70 °C, 48 h) are required for the generation of Ir(III) species, and even then the extent of additional ligand activation is confined to a single C-H bond. The product so formed, $\text{Ir}(5\text{-Mes})(5\text{-Mes}')\text{HCl}$ (**3**) is reminiscent of the products of the reactions of M(I) precursors (M = Rh, Ir)^{6(e),7} with the unsaturated imidazolylidene ligand, IMes.



Scheme 1 Syntheses of 5- and 6-Mes complexes of iridium **1-3**. Key reagents and conditions: (i) $[\text{Ir}(\text{COE})_2\text{Cl}]_2$ (0.166 equiv.), THF, 20 °C, 12 h, 52%; (ii) $[\text{Ir}(\text{COE})_2\text{Cl}]_2$ (0.25 equiv.), THF, 20 °C, 12 h, 82%; (iii) toluene, 70 °C, 24 h, 79%.

The higher (effective C_2) symmetry implicit in the doubly activated systems **1** and **1'** (*cf.* mono-activated **3**) is reflected in the respective ^1H NMR spectra (e.g. three *ortho*-Me and two *para*-Me signals for **1** *cf.* four *ortho*-Me and three *para*-Me for **3**). In each of the Ir(III) compounds, the presence of the hydride ligand is signaled by a very high field ^1H NMR resonance (at $\delta_{\text{H}} = -37.54$, -36.85 and -32.85 ppm for **1**, **1'** and **3**, respectively). Such chemical shifts are also consistent with the solid-state structures determined crystallographically [Figure 1 and reference 6(h)], which feature in each case, a heavy atom skeleton defining an approximately planar co-ordination environment at iridium, with the hydride ligand being located effectively *trans* to a vacant site.⁸

The differing reactivity of the 5-Mes and 6-Mes NHCs towards $[\text{Ir}(\text{COE})_2(\mu\text{-Cl})]_2$, generating (at room temperature) Ir(I) and Ir(III) systems, respectively, is consistent with the electronic properties of the two ligands. Thus, saturated 6-membered NHCs are known to be appreciably more basic than their 5-membered analogues,^{3(e)} and presumably therefore render the iridium centre more susceptible to oxidative addition. The steric profiles of the two ligands are evidently less important here, since, although the extra backbone methylene group in 6-Mes pushes the N-bound mesityl groups

further towards the metal centre, it is evident from the crystal structure of **3**, for example, that C-H activation of an *ortho*-methyl group in the 5-Mes ligand can occur without introducing undue strain into the system. Thus, the Ir-C(carbene) distance associated with the activated NHC ligand in **3** [2.022(5) Å] is, if anything, shorter than the corresponding distance involving the unactivated 5-Mes ligand [2.049(3) Å]. Moreover the ‘canting’ of the NHC heterocycle to one side to accommodate the benzylic tether [as manifested by Ir(1)-C(11)-N angles of 123.6(3) and 128.7(3)°] is not noticeably different from the asymmetry implicit in the binding of the *unactivated* NHC in the same compound [*cf.* Ir(1)-C(26)-N angles of 124.6(3) and 128.2(3)°].

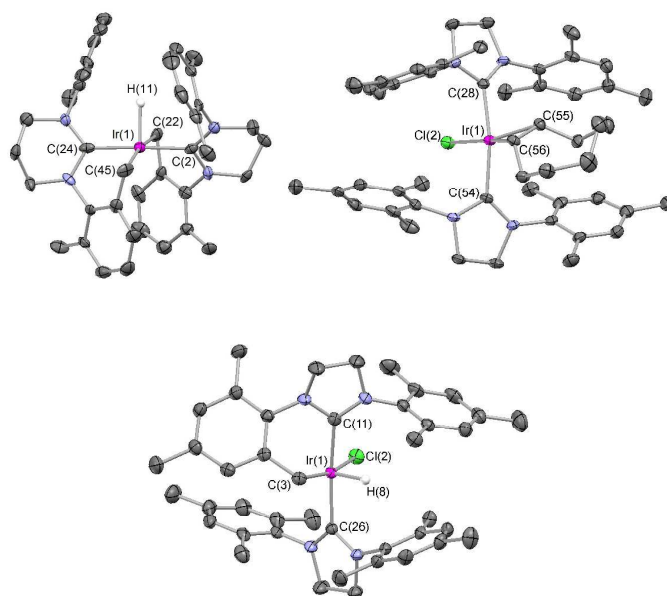
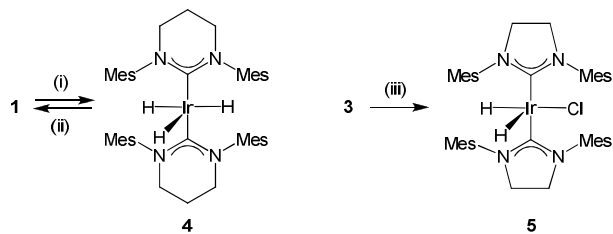


Figure 1 Molecular structures of (top left) $\text{Ir}(6\text{-Xyl})_2\text{H}$ (**1'**), (top right) $\text{Ir}(5\text{-Mes})_2(\text{COE})\text{Cl}$ (**2**) and (bottom) $\text{Ir}(5\text{-Mes})(5\text{-Mes}')\text{HCl}$ (**3**) as determined by X-ray crystallography; most hydrogen atoms omitted for clarity and thermal ellipsoids set at the 40% probability level. Key bond lengths (Å) and angles (°): (for **1'**) Ir(1)-C(2) 1.98(1), Ir(1)-C(24) 2.00(1), Ir(1)-C(22) 2.161(9), Ir(1)-C(45) 2.096(9), Ir(1)-H(11) 1.68, C(2)-Ir(1)-C(24) 177.5(5), C(22)-Ir(1)-C(45) 167.8(4); (for **2**) Ir(1)-Cl(2) 2.367(1), Ir(1)-C(28) 2.061(4), Ir(1)-C(54) 2.076(4), Ir(1)-C(55) 2.135(5), Ir(1)-C(56) 2.130(5), C(55)-C(56) 1.427(7); (for **3**) Ir(1)-Cl(2) 2.415(1), Ir(1)-C(3) 2.099(4), Ir(1)-C(11) 2.022(5), Ir(1)-C(26) 2.049(3), Ir(1)-H(8) 1.52, Cl(2)-Ir(1)-C(3) 167.3(1), C(11)-Ir(1)-C(26) 173.1(2).

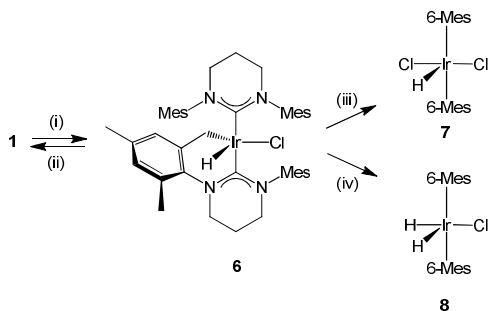
Reversal of C-H activation chemistry via reactions with HX

While, ultimately, extrusion of the alkene ligands from $[\text{Ir}(\text{COE})_2(\mu\text{-Cl})]_2$ by either 5-Mes and 6-Mes appears to implicate activation of one or more pendant mesityl groups, subsequent reaction of the C-H activated products with reagents of the type HX offers a versatile route back to simple C(2) bound *bis*(NHC) complexes. Thus, for example, the reaction of **3** with dihydrogen leads to quantitative conversion by ^1H NMR to $\text{Ir}(5\text{-Mes})_2(\text{H}_2)\text{Cl}$ (**5**; Scheme 2), while the corresponding reaction with **1** yields a complex of overall composition $\text{Ir}(6\text{-Mes})_2\text{H}_3$ (**4**).



Scheme 2 Hydrogenation of 5- and 6-Mes complexes **1** and **3**. Key reagents and conditions: (i) H₂ (4 atm.), toluene, 20 °C, 5 h, quantitative; (ii) vacuum, 20 °C, 4 d, ca. 25%; or TBE, 20 °C, 16 h, quantitative; (iii) H₂ (4 atm.), toluene, 20 °C, 1 h, quantitative.

Additionally, in the case of **1**, *stepwise* cleavage of the two Ir-C bonds can be effected via reactions with stoichiometric quantities of HCl (Scheme 3). Thus, reaction with a single equivalent of the acid leads to controlled formation of Ir(6-Mes)(6-Mes')HCl (**6**), i.e. the 6-Mes analogue of compound **3**. **6** is a potential intermediate in the initial synthesis of Ir(6-Mes')₂H (**1**) from 6-Mes and [Ir(COE)₂(μ-Cl)]₂, with subsequent loss of HCl (driven by the presence of excess NHC acting as a base) presumably facilitating a second C-H activation step. Consistently, reaction of **6** with one equivalent of 6-Mes leads to the regeneration of the doubly activated system **1**.



Scheme 3 Hydrogenation of 5- and 6-Mes complexes **1** and **3**. Key reagents and conditions: (i) HCl (1.0 equiv.), Et₂O, 20 °C, 30 min, 90%; (ii) 6-Mes, benzene-d₆, quantitative by ¹H NMR; (iii) HCl (1.0 equiv.), Et₂O, 20 °C, 30 min, 83%; (iv) H₂ (3 atm), toluene, 20 °C, 3 h, 84%.

Reaction of **6** with a second equivalent of HCl leads to protonation of the single remaining iridium benzyl function, and to the formation of the *bis*(6-Mes) stabilized (hydrido)-iridium dichloride species **7**. Alternatively, the reaction of **6** with dihydrogen allows access to the corresponding (dihydrido)iridium chloride species **8**, thereby completing access to a range of systems of the type Ir(6-Mes)₂H_{*n*}Cl_{3-*n*} (*n* = 1 - 3).

The characterization of mixed hydrido/chloride complexes **5-8** relies heavily on multinuclear NMR spectroscopy and mass spectrometry, allied to X-ray crystallography for compounds **5** and **8** (Figure 2). In the case of compound **6**, which retains a single benzylic tether, a 2:1:1 pattern is observed for the aromatic *meta*-CHs of the activated NHC, together with three *ortho*-methyl signals (3:3:3) and two mutually coupled doublets (at δ_H = 2.19, 2.30 ppm, ²J_{HH} = 11.5 Hz) assigned to the IrCH₂ unit. In addition, a high-field signal at δ_C = -13.2 ppm displaying a two-bond coupling to the metal-bound hydride (²J_{CH} = 10.1 Hz) is assigned to the IrCH₂ unit in the ¹³C NMR

spectrum. This spectrum also features two carbene signals at δ_C = 207.7 and 204.0 ppm, consistent with the presence of both activated 6-Mes' and unactivated 6-Mes donors. Similar patterns of resonances are observed in the corresponding spectra of the structurally characterized 5-Mes analogue, **3**. That said, the Ir-H resonance measured for **6** (δ_H = -46.50 ppm) is shifted significantly upfield compared to that of **3** (δ_H = -32.85 ppm), consistent with the stronger σ-donating capabilities of the six-membered heterocycle.^{3e}

By contrast, hydrido/dichloride and dihydrido/chloride species **5**, **7** and **8** display much simpler ¹H and ¹³C NMR spectra, consistent with the presence of unactivated NHC substituents. Thus, in each case, a pattern consisting of one aromatic *meta*-CH (8H), one *ortho*-methyl (24H) and one *para*-methyl signal (12H) is observed, together with a very high field resonance associated with the metal-bound hydride ligand [at δ_H = -32.81 (**5**), -49.80 (**7**) and -33.50 ppm (**8**)]. The structures of compounds **5** and **8** have been determined by X-ray crystallography (Figure 2) and confirm the heavy-atom skeletons predicted spectroscopically. It is of note that the Ir-C(carbene) distances measured for the 6-Mes system **8** [2.053(3) Å] are markedly longer than those determined for its like-for-like 5-Mes counterpart **5** [2.009(6), 2.016(6) Å]. Such a trend presumably reflects not only the increased steric demands of the flanking aryl substituents (%V_{bur} = 36.1, 44.0 for 5-Mes and 6-Mes, respectively, based on their LAuCl complexes),^{4(f),5} but also the greater C 2p orbital character in the carbene lone pair as the N-C-N angle widens.^{1b}

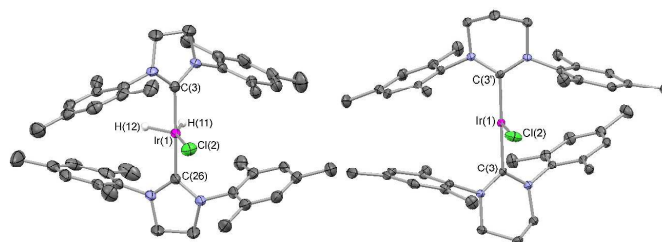


Figure 2 Molecular structures of Ir(5-Mes)₂(H)₂Cl (**5**) and the heavy atom skeleton of Ir(6-Mes)₂(H)₂Cl (**8**) as determined by X-ray crystallography; most hydrogen atoms omitted for clarity and thermal ellipsoids set at the 40% probability level. Key bond lengths (Å) and angles (°): (for **5**) Ir(1)-Cl(2) 2.404(2), Ir(1)-C(3) 2.016(6), Ir(1)-C(26) 2.009(6), Ir(1)-H(11) 1.53, Ir(1)-H(12) 1.60, C(3)-Ir(1)-C(26) 176.5(2); (for **8**) Ir(1)-Cl(2) 2.401(2), Ir(1)-C(3) 2.053(3), C(3)-Ir(1)-C(3') 177.5(1).

In contrast to the very high field resonances associated with the hydride ligands in the mixed hydrido/chloride systems **7** and **8** (-49.80 and -33.50 ppm, respectively), the corresponding signal for Ir(6-Mes)₂H₃ (**4**) is located at δ_H = -9.75 ppm. **4** is also found to be stable only under an atmosphere of dihydrogen. Purging the system, either by placing under continuous vacuum, or by replacement of the H₂ overpressure with argon leads to the observation of multiple hydride signals in the ¹H NMR spectrum, including that of doubly C-H activated system **1**. Cleaner dehydrogenative conversion of **4** back to **1** can be achieved over a 12 h period by the addition of *tert*-butylethylene (TBE, 3,3-dimethylbutene; Scheme 2). Crystals of **4** suitable for X-ray crystallography could be

obtained by re-crystallization under a dihydrogen atmosphere, but even then the quality of the solution was poor and only sufficient to confirm the heavy atom skeleton and a linear C-Ir-C array.

Exposure of **4** to excess D₂ (at ca. 4 atm pressure) leads to incorporation into the Ir-H position, such that the hydride resonance in the ¹H NMR spectrum completely disappears over a period of ca. 14 days. At shorter reaction times the signal is observed to broaden, although no distinct signals could be resolved attributable to the isotopic perturbation of chemical shift potentially observed for an IrL₂(H₂)H formulation.⁹ Deuterium exchange into the high field signal also appears to be correlated with its incorporation into the *ortho*-methyl positions of the 6-Mes ligand, an observation consistent (i) with the observed reconversion of **4** to C-H activated Ir(6-Mes)₂H (**1**) under continuous vacuum, and (ii) with a proposed mechanism in which elimination of H₂ from **4** is rapidly followed by (or even synchronous with) intramolecular C-H activation.

The nature of the hydride ligands in **4** was further investigated by VT-NMR experiments. Low temperature ¹H NMR measurements in toluene-d₈ do not reveal any evidence of decoalescence in the high field signal at the lowest temperature accessed (193 K). The measured value of T₁(min), 510 ms (at 300 MHz and 253 K) is comparable to (or even greater than) those determined for classical Ir(III) hydrides [e.g. 215 ms at 400 MHz and 233 K for Ir(PCy₃)₂(H)₂(κ²-S₂CH)], but markedly in excess of that determined for the rapidly exchanging hydride/dihydrogen ligands in the related cation [Ir(PCy₃)₂(H)(H₂)(κ²-S₂CH)]⁺ (29 ms at 400 MHz and 213 K).^{10,11} As such, these data are certainly more consistent with an Ir(III) trihydride formulation for **4**, Ir(6-Mes)₂(H)₃, rather than an Ir(I) hydride(dihydrogen) structure. Of interest spectroscopically, then, is the markedly lower field ¹H chemical shift associated with the three (rapidly exchanging) hydride ligands in **4**, compared to those for the mixed hydride/chloride species **7** and **8** (Figure 3). The lowest energy structure calculated by DFT for the model trihydride Ir(6-Me)₂(H)₃ features an approximately square pyramidal coordination geometry, reminiscent of those determined crystallographically for **1**, **1'** and **3**, and in line with that predicted computationally by Eisenstein and co-workers for the model *bis*(phosphine) system Ir(PH₃)₂(H)₃.¹² Such a geometry features two distinct hydride ligand environments, either *trans* to a vacant site, or to another hydride. Hydride ligands in Ir(III) systems situated opposite vacant coordination sites are known to give rise to

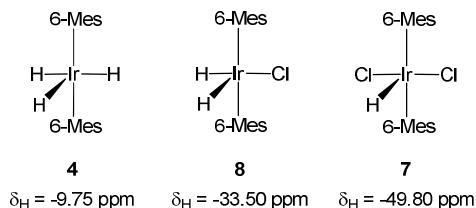
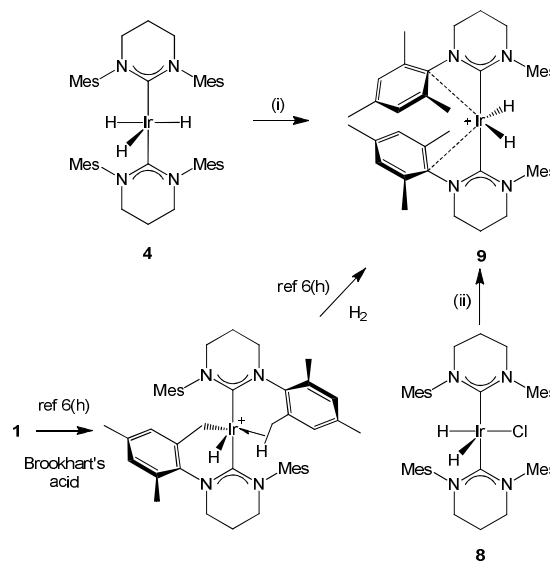


Figure 3 ¹H NMR shifts for the iridium hydride ligands in complexes of the type Ir(6-Mes)₂H_nCl_{3-n} (n = 1 - 3).

very high field chemical shifts ($\delta_{\text{H}} < -40$ ppm),^{8(b)} and that measured for **7** (-49.80 ppm) is therefore consistent with the proposed square pyramidal geometry (Figure 3). In the case of **4**, however, the single fluxionally-averaged resonance presumably reflects the weighted mean of an analogous very high field signal, and a lower field signal due to the *trans*-IrH₂ unit. Brookhart, for example, has recently shown that *trans*-Ir(III)H₂ units give rise to much lower field ¹H resonances [e.g. $\delta_{\text{H}} = -9.07$ ppm for the hydride ligands in (PONOP)Ir(CH₃)(H)₂].^{13,14}

Synthesis and reactivity of cationic systems of the type [Ir(NHC)₂(H)₂]⁺

In preliminary work we showed that the reaction of **1** with the conjugate acid of a very weakly basic anion (e.g. [H(OEt₂)₂][BAR₄⁻], Brookhart's acid) leads to the protonation of one of the benzyl functions and to the formation of [Ir(6-Mes)(6-Mes')H]⁺ in which the formally 14-electron metal centre is stabilized not by the anion but by a (highly fluxional) agostic interaction (Scheme 4).^{6(h)} Subsequent reaction of [Ir(6-Mes)(6-Mes')H]⁺ with dihydrogen, proceeds in much the same way as the hydrogenation of **6** to **8**, generating in this case the cationic dihydride [Ir(6-Mes)₂(H)₂]⁺ (**9**) which features no significant interaction with the [BAR₄⁻] counter-ion.^{6(h)} However, in view of the syntheses described above of a number of alternative potential precursors [of the type Ir(6-Mes)₂(H)₂X], we have sought to open up more convenient synthetic routes to such 14-electron dihydride systems (Scheme 4).



Scheme 4 Generation of the [Ir(6-Mes)₂(H)₂]⁺ cation via hydride or halide abstraction ([BAR₄⁻] counter-ions omitted for clarity). Key reagents and conditions: (i) [Ph₃C][BAR₄⁻] (1.0 equiv.), fluorobenzene, -30 °C, 2 h, 54%; (ii) Na[BAR₄⁻] (1.0 equiv.), fluorobenzene, -30 °C, 2 h, 78%.

In the event, the reaction of either Ir(6-Mes)₂(H)₃ (**4**) with a hydride abstraction agent such as [Ph₃C][BAR₄⁻], or of Ir(6-Mes)₂(H)₂Cl (**8**) with the halide abstractor Na[BAR₄⁻], provides facile access to [Ir(6-Mes)₂(H)₂][BAR₄⁻]. Similar chemistry can be shown to generate the related 6-Xyl derivative [Ir(6-

Xyl)₂(H)₂][BAR^f₄] (**9'**), but attempts to isolate the corresponding 5-Mes complex via analogous routes have proved unsuccessful. Thus, for example, halide abstraction protocols appear to generate systems featuring Ir-F bonds, presumably via fluoride abstraction from the [BAR^f₄]⁻ counter-ion by a highly electrophilic species. In stark contrast, **9** and **9'** are extraordinarily robust systems, being stable to exposure to both air and moisture, and able to be re-crystallized unchanged from bench (i.e. wet) chloroform in air over a period of >10 days.

Crystallographic studies of both **9** and **9'** reveal the underlying origins of this inertness. In each case, the putative 14-electron metal centre is stabilized by additional interactions involving the π-systems of flanking aryl rings. Thus, in the case of **9'**, for example (Figure 4), contacts between the iridium centre and *ipso*-carbons of two of the flanking xylyl groups [2.809(5), 2.818(7) Å] are comfortably within the sum of the respective van der Waals radii (3.87 Å).¹⁵ While some distortion of the metal-carbene fragment is required to bring about this secondary ligation at Ir(1) – as manifested by divergent Ir(1)-C(2)-N angles [129.4(5) and 112.9(5)°] – it is clear from a spacing filling representation of the structure of [Ir(6-Xyl)₂(H)₂]⁺ that the resulting alignment of the two flanking xylyl rings very effectively shields the coordination environment of the metal centre *trans* to the hydride ligands. In addition, it is apparent from this depiction that the steric 'shrouding' relies very little on the presence (or otherwise) of the *para*-methyl groups, consistent with the similar inertness observed for both **9** and **9'**. By contrast, the markedly narrower NCN angle associated with a coordinated 5-Mes heterocycle [e.g. 106.2(4)° for **5**, cf. 115.1(3)° for **8**] presumably means that the corresponding degree of aryl π-stabilization and steric protection of the metal centre in the putative [Ir(5-Mes)₂(H)₂]⁺ cation will be significantly reduced.

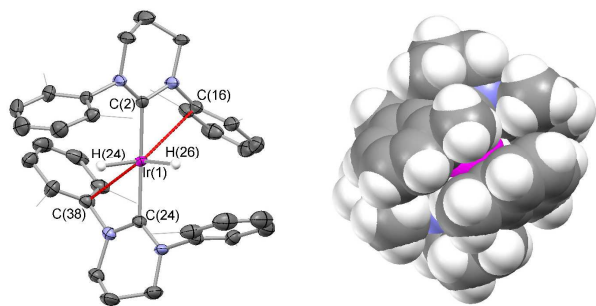


Figure 4 Two views of the molecular structure of [Ir(6-Xyl)₂(H)₂][BAR^f₄] (**9'**) as determined by X-ray crystallography. (Left) thermal ellipsoid plot (40% probability level); most hydrogen atoms omitted and xylyl methyl groups shown in wireframe format for clarity; contacts between Ir(1) and xylyl *ipso* carbons shown in red. (Right) space filling representation. Key bond lengths (Å) and angles (°): Ir(1)-C(2) 2.042(6), Ir(1)-C(24) 2.049(6), Ir(1)-H(24) 1.68, Ir(1)-H(26) 1.72, Ir(1)-C(16) 2.818(7), Ir(1)-C(38) 2.809(5), C(2)-Ir(1)-C(24) 176.1(3).

While the exploitation of 6-Mes/6-Xyl ligands in these systems gives rise to 'bottle-able' air-stable formally 14-electron cations, a related consequence is a lack of affinity of complexes such as **9/9'** towards external B-H/N-H containing substrates. Thus, even in the presence of excess H₃BNMe₃ or

H₃BNMe₂H, no evidence is seen for coordination or activation of these substrates. By contrast, the much more labile [Ir(5-Mes)₂(H)₂]⁺ system, while not isolable (at least in our hands), can be accessed *in situ* and trapped by coordination of the amineborane H₃BNMe₃. Thus, addition of a 1:1 mixture of **5** and H₃BNMe₃ in THF to a suspension of Na[BAR^f₄] leads to the formation of [Ir(5-Mes)₂(H)₂(κ²-H₃BNMe₃)] [BAR^f₄] (**10**), the identity of which is suggested by ¹H NMR signals assigned to the IrH₂ (δ_H = -21.86 ppm) and fluxional BH₃ moieties (δ_H = -2.11 ppm), and by an ¹¹B signal at δ_B = 13.0 ppm. The corresponding signals for the related IMes system, [Ir(IMes)₂(H)₂(κ²-H₃BNMe₃)] [BAR^f₄], are found at -21.80, -2.28 and 14.4 ppm, respectively.^{6(c)} The structure of **10** in the solid state has also been determined by X-ray crystallography (Figure 5), which confirms that the elusive [Ir(5-Mes)₂(H)₂]⁺ fragment has indeed been trapped by coordination of the H₃BNMe₃ ligand, acting as a 4-electron κ²-ligand. Structural metrics for the cationic component of **10** [notably the Ir-B and B-N distances of 2.24(1)/1.55(2) Å, and the Ir-B-N angle of 138.5(7)°] are close to those determined for the imidazolylidene analogue.^{6(c)}

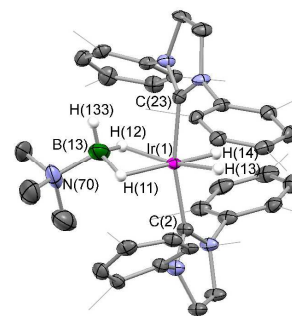


Figure 5 Molecular structures of the cationic component of [Ir(5-Mes)₂(H)₂(κ²-H₃BNMe₃)] [BAR^f₄] (**10**) as determined by X-ray crystallography; most hydrogen atoms omitted and mesityl methyl groups shown in wireframe format for clarity. Thermal ellipsoids set at the 40% probability level. Key bond lengths (Å) and angles (°): Ir(1)-C(2) 2.039(7), Ir(1)-C(23) 2.040(7), Ir(1)-B(13) 2.24(1), B(13)-N(70) 1.55(2), C(2)-Ir(1)-C(23) 166.2(3), Ir(1)-B(13)-N(70) 138.5(7).

14-Electron systems of the type [ML₂(H)₂]⁺ (M = Rh, Ir) have also been shown to be active catalysts for the dehydrogenation of a range of B/N containing substrates,^{6(b),6(c),16} and in a similar vein, *in situ* generated [Ir(5-Mes)₂(H)₂]⁺ can be shown to be competent for the conversion of H₃BNMe₂H to (H₂BNMe₂)₂ in THF. In this case, the metal-containing product isolated after 1 h is shown by multinuclear NMR and a combination of X-ray and neutron diffraction studies to be a co-crystallite of the amineborane adduct [Ir(5-Mes)₂(H)₂(κ²-H₃BNMe₂H)] [BAR^f₄] (**11**) and the corresponding complex of the dehydrogenated aminoborane ligand H₂BNMe₂, i.e. [Ir(5-Mes)₂(H)₂(κ²-H₂BNMe₂)] [BAR^f₄] (**12**) in a ratio of ca. 4:6 (Figure 6 and Table 1).^{6(b),6(c),17} The co-crystallization of these two complexes presumably reflects the very similar binding affinities of κ²-H₂BNMe₂ and H₃BNMe₂H ligands determined computationally.¹⁸

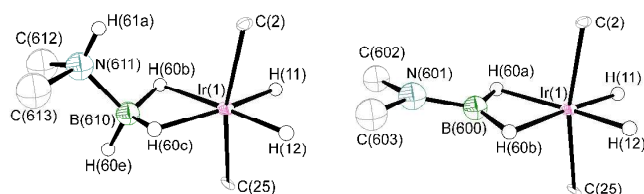


Figure 6 Key aspects of the iridium coordination spheres of $[\text{Ir}(5\text{-Mes})_2(\text{H})_2(\kappa^2\text{-H}_3\text{BNMe}_2\text{H})][\text{BARf}_4]$ (**11**) and $[\text{Ir}(5\text{-Mes})_2(\text{H})_2(\kappa^2\text{-H}_2\text{BNMe}_2)][\text{BARf}_4]$ (**12**) as determined by single crystal neutron diffraction. Thermal ellipsoids set at the 40% probability level.

Table 1 Key structural metrics relating to amine- and aminoborane coordination to $[\text{Ir}(5\text{-Mes})(\text{H})_2]^+$ obtained from neutron diffraction studies of **11** and **12**.

Parameter ^a	11	12
$d(\text{Ir}\cdots\text{B})$	2.21(4)	2.07(2)
$d(\text{B}\cdots\text{N})$	1.55(3)	1.40(2)
$d(\text{N}\cdots\text{C})$	1.54(3), 1.51(3)	1.51(2), 1.51(2)
$d(\text{N}\cdots\text{H})$	0.98(6)	-
$d(\text{B}\cdots\text{H}_i)$	1.13(6)	-
$d(\text{B}\cdots\text{H}_b)$	1.21(6), 1.29(8)	1.28(3), 1.33(4)
$d(\text{Ir}\cdots\text{H}_b)$	1.75(7), 1.87(6)	1.83(3), 1.87(3)
$\angle(\text{Ir}\cdots\text{B}\cdots\text{N})$	125(2)	171(1)
$d(\text{Ir}\cdots\text{H}_i)$	1.53(2), 1.54(2)	
$d(\text{Ir}\cdots\text{C})$	2.035(7), 2.043(6)	
$\angle(\text{C}\cdots\text{Ir}\cdots\text{C})$	167.6(3)	

^aDistances in Å, angles in degrees.

The structure determined by neutron diffraction for the aminoborane complex component (i.e. **12**) has much in common with that reported for the analogous IMes system – which has been characterized by the same technique.^{6d} Thus, both the IMes and 5-Mes systems feature a close-to-linear $\text{Ir}\cdots\text{B}\cdots\text{N}$ framework, and the metrics associated with the $\text{Ir}(\mu\text{-H})_2\text{B}$ unit are also very similar for the two complexes [e.g. $d(\text{Ir}\cdots\text{B}) = 2.07(2)$ for **12** vs. $2.044(11)$ Å; $d(\text{Ir}\cdots\text{H}_b) = 1.83(3)/1.87(3)$ vs. $1.886(16)/1.822(19)$ Å and $d(\text{B}\cdots\text{H}_b) = 1.28(3)/1.33(4)$ vs. $1.30(2)/1.41(2)$ Å]. The structure of aminoborane complex **11**, on the other hand, represents to our knowledge, the first to be determined for such a system by neutron diffraction. The non-linear $\text{Ir}\cdots\text{B}\cdots\text{N}$ unit, and longer $\text{Ir}\cdots\text{B}$ and $\text{B}\cdots\text{N}$ separations (cf. **12**) are consistent with the results of X-ray studies of complexes featuring four-coordinate aminoborane ligands [cf. $138.5(7)^\circ$, $2.24(1)$, $1.55(2)$ Å for **10**]. The $\text{Ir}(\mu\text{-H})_2\text{B}$ unit defining the κ^2 mode of coordination is, however very similar to that found in **12**, being essentially planar, and featuring $\text{Ir}\cdots(\mu\text{-H})$ and $\text{B}\cdots(\mu\text{-H})$ distances of $1.75(7)/1.87(6)$ and $1.21(6)/1.29(8)$ Å, respectively.

Conclusions

The differing steric and electronic properties of the 5- and 6-Mes NHC ligands have been illuminated through their reactivity in a number of iridium systems. Both ligands possess an array of readily accessible *ortho*-methyl C-H bonds, and their differing reactivities towards $[\text{Ir}(\text{COE})_2(\mu\text{-Cl})_2]$ - generating Ir(I) and Ir(III) complexes, respectively -

presumably reflects the stronger σ -donor characteristics of the expanded ring system. Thus, under more forcing conditions, the 5-Mes system can be shown to be amenable to similar C-H activation processes without appearing to introduce significant strain in the resulting chelate ring.

While σ -donor capabilities might also be expected to play a role in modulating the lability of the related (formally 14-electron) cations $[\text{IrL}_2(\text{H})_2]^+$, the starkly differing properties of $[\text{Ir}(5\text{-Mes})_2(\text{H})_2]^+$ and $[\text{Ir}(6\text{-Mes})_2(\text{H})_2]^+ / [\text{Ir}(6\text{-Xyl})_2(\text{H})_2]^+$ are also thought to be influenced by the closer approach of the pendant aryl substituents to the unsaturated metal centre in the latter case. Thus, additional (albeit weak) stabilization of the metal centre through interaction with the aryl π -system is facilitated for the 6-membered heterocycles by the wider N-C-N angle and consequent closing up of the cavity defined by the flanking substituents. The packing of the aryl groups around the metal centre which leads to highly effective screening from external reagents – a factor which is responsible not only for the remarkable lack of reactivity of 6-Mes derivative **9** towards air and moisture, but also to its lack of catalytic activity in aminoborane dehydrogenation. The role of the *para*-methyl groups in controlling this inertness appears to be minor, with similar reactivity (or lack thereof) being observed for the *ortho*-xyllyl analogue **9'**.

Experimental

General considerations: All manipulations were carried out using standard Schlenk line or dry-box techniques under an atmosphere of argon. With the exception of fluorobenzene, solvents were degassed by sparging with argon and dried by passing through a column of the appropriate drying agent using a commercially available Braun SPS; fluorobenzene was dried by refluxing over calcium hydride, distilled, sparged and stored over activated molecular sieves. NMR spectra were measured in C_6D_6 or CD_2Cl_2 which were dried over potassium or molecular sieves, respectively, and stored under argon in Teflon valve ampoules. NMR samples were prepared under argon in 5 mm Wilmad 507-PP tubes fitted with J. Young Teflon valves. ^1H and ^{13}C NMR spectra were recorded on Varian Mercury-VX-300 or Bruker AVII-500 spectrometers and referenced internally to residual protio-solvent (^1H) or solvent (^{13}C) resonances and are reported relative to tetramethylsilane ($\delta = 0$ ppm). ^{11}B and ^{19}F NMR spectra were referenced with respect to $\text{Et}_2\text{O}\cdot\text{BF}_3$ and CFCl_3 , respectively. Chemical shifts are quoted in δ (ppm) and coupling constants in Hz. Elemental analyses were carried out at London Metropolitan University. Starting materials 5-Mes (sIMes),¹⁹ 6-Xyl,^{3(a)} 6Mes,^{3(a)} $[\text{Ir}(\text{COE})_2(\mu\text{-Cl})_2]$,²⁰ $\text{Na}[\text{BARf}_4]$,²¹ $[\text{H}(\text{OEt})_2][\text{BARf}_4]$,²² and $[\text{Ph}_3\text{C}][\text{BARf}_4]$ ²³ were prepared by literature procedures. The syntheses of complexes **1** and **9** have been communicated by us previously.^{6(h)}

Crystallography: Single crystal X-ray diffraction data for compounds were collected on a Nonius KappaCCD (compounds **1'**, $2'\text{OEt}_2$, **3**, **5**, **9'**, **10** and **11/12**) or Oxford Diffraction SuperNova diffractometer (compound **8**) at 150 K (100 K for **11/12**). Data collection and reduction were carried out using Collect and Denzo/Scalepack or CrysAlis, respectively. The structures were solved using either Sir92 or Superflip and refined using CRYSTALS.²⁴ Hydrogen atoms

were generally visible in the difference map and were refined with restraints before inclusion in the final refinement using a riding model.^{24(d)} The Flack x parameter was refined for the non-centrosymmetric cases,^{24(e),25} except for **1'** which was also twinned by rotation about the a -axis.²⁶ PLATON/SQUEEZE was used to deal with diffuse residual electron density in the voids in **3**.²⁷ Single crystal neutron diffraction data were collected at 100 K on the time-of-flight Laue diffractometer SXD at the ISIS spallation neutron source.²⁸ The X-ray structure solution was refined against the neutron diffraction data using SHELXL.²⁹ Complete details of all structures are contained within the respective CIFs which have been deposited with the CCDC (1002300-1002308).

Syntheses: *Ir(6-Xyl)₂H (1')*. A solution of 6-Xyl (350 mg, 1.20 mmol) in THF (20 mL) was added to a stirred solution of [Ir(COE)₂(μ -Cl)]₂ (257 mg, 0.287 mmol) also in THF (20 mL). The reaction mixture was stirred at room temperature for 12 h and darkened to an orange/brown. Removal of the volatiles in vacuo yielded a dark orange solid, which was washed hexanes (3 x 15 mL) and extracted into toluene. Layering of the toluene solution with pentane and storage at -30 °C gave red crystals suitable for X-ray crystallography in 43% yield (190 mg). ¹H NMR (C₆D₆, 300 MHz, 298 K): δ_{H} 7.22 (2H, d, ³ J_{HH} = 9.0 Hz, *meta*-H Xyl), 7.11 (2H, t, ³ J_{HH} = 9.0 Hz, *para*-H Xyl), 7.06 (2H, d, ³ J_{HH} = 6.0 Hz, *meta*-H Xyl'), 6.90 (2H, t, ³ J_{HH} = 6.0 Hz, *para*-H Xyl'), 6.68, 6.12 (2H, d, ³ J_{HH} = 6.0 Hz, *meta*-H Xyl'), 3.10 (2H, m, NCH₂), 2.73 (2H, m, NCH₂), 2.60 (4H, m, NCH₂), 2.38 (6H, s, *ortho*-CH₃), 2.20 (6H, s, *ortho*-CH₃), 2.13 (2H, d, ² J_{HH} = 6.3 Hz, IrCH₂), 2.00 (2H, d, ² J_{HH} = 6.3 Hz, IrCH₂), 1.85 (6H, s, *ortho*-CH₃), 1.43 (4H, m, NCH₂CH₂), -36.85 (1H, s, IrH). ¹³C NMR (C₆D₆, 126 MHz, 298 K): δ_{C} 203.8 (NCN), 147.4 (NC Xyl), 144.8 (NC Xyl'), 137.0 (*ortho*-C Xyl), 135.5 (*ortho*-C Xyl'), 130.2 (*meta*-CH Xyl), 128.7 (*meta*-CH Xyl'), 127.5 (*meta*-CH Xyl'), 126.6 (*para*-CH Xyl), 125.5 (*ortho*-CH Xyl'), 123.2 (*para*-CH Xyl'), 47.9 (NCH₂), 46.1 (NCH₂), 22.9 (NCH₂CH₂), 20.1 (*ortho*-CH₃ Xyl'), 18.7 (*ortho*-CH₃ Xyl), 15.6 (*ortho*-CH₃ Xyl'), 7.8 (IrCH₂). MS (EI +ve): m/z (%) 774.4 (10) [M-2H]⁺, 776.4 (5) M⁺. Accurate mass ([C₄₀H₄₅N₄¹⁹¹Ir]⁺): 772.3238 (meas.), 772.3272 (calc.). Elemental analysis (meas.): C 61.78; H 5.93; N 7.12. (calc.): C 61.99; H 5.98; N 7.23. Crystallography (for **1'**): C₄₀H₄₆IrN₄, M_r = 775.03, monoclinic, $P2_1$, a = 9.0172(3), b = 15.0295(6), c = 12.2995(5) Å, β = 94.952(2)°, V = 1660.6(1) Å³, Z = 2, ρ_c = 1.550 Mg m⁻³, T = 150 K, λ = 0.71073 Å, 15631 reflections collected, 7051 independent [R(int) = 0.090], which were used in calculations. R_1 = 0.0492, wR_2 = 0.0832 for observed unique reflections [$I > 2\sigma(I)$] and R_1 = 0.0877, wR_2 = 0.0946 for all unique reflections. Max. and min. residual electron densities 6.96 and -5.76 e Å⁻³. CCDC ref.: 1002300.

(5-Mes)₂Ir(COE)Cl (2). A solution of 5-Mes (274 mg, 2.6 mmol) in THF (30 mL) was added to a stirred solution of [Ir(COE)₂(μ -Cl)]₂ (200 mg, 0.22 mmol) also in THF (20 mL). The orange solution was stirred for 12 h and darkened to an orange/brown colour. Removal of the volatiles in vacuo yielded an orange solid which was extracted into diethyl ether (3 x 30 mL). Concentration and storage at -30 °C produced orange crystals in 82% yield (370 mg). Crystals of 2'OEt₂ suitable for X-ray crystallography were obtained by slow evaporation of a diethyl ether solution at room temperature. ¹H NMR (C₆D₆, 300 MHz, 298 K): δ_{H} 6.96 (2H, s, *meta*-CH Mes), 6.84 (6H, s, *meta*-CH Mes), 3.16 (4H, m, NCH₂), 3.08 (4H, m, NCH₂), 2.55 (6H, s, *para*-CH₃), 2.47 (6H, s, *para*-CH₃), 2.32 (6H, s, *ortho*-CH₃), 2.29 (6H, s, *ortho*-CH₃), 2.24 (6H, s, *ortho*-CH₃), 2.20 (6H, s, *ortho*-

CH₃), 2.06 (2H, dd, ³ J_{HH} = 9.6 Hz, CH COE), 1.73, 1.38, 1.23 (each 4H, m, CH₂ COE). ¹³C NMR (C₆D₆, 75 MHz, 298 K): δ_{C} 207.9, 204.0 (NCN), 138.7, 137.7 (NC Mes), 137.4, 137.3 (*para*-C Mes), 134.8, 134.3, 134.1, 133.7 (*ortho*-C Mes), 128.9, 128.5, 128.2, 127.6 (*meta*-CH Mes), 51.1, 49.6 (NCH₂), 36.5 (CH COE), 30.1, 27.1, 26.3 (CH₂ COE), 20.8, 19.8 (*para*-CH₃), 19.4, 18.7, 18.0, 17.3 (*ortho*-CH₃). MS (EI +ve): m/z (%) 950.5 (4) M⁺. Accurate mass ([C₅₀H₆₆N₄¹⁹¹IrCl]⁺): 948.4574 (meas.), 948.4581 (calc.). Reproducible elemental microanalysis for **2** proved difficult to obtain due to the retention of variable amounts of diethyl ether solvate. While attempts to obtain crystalline samples from alternative solvents were unsuccessful, ¹H and ¹³C NMR data imply that bulk samples were >95% pure. Crystallography (for 2'OEt₂): C₅₄H₇₆ClIrN₄O, M_r = 1024.90, monoclinic, $P2_1/c$, a = 17.3193(2), b = 18.8464(2), c = 15.1207(1) Å, V = 4908.4(1) Å³, Z = 4, ρ_c = 1.387 Mg m⁻³, T = 150 K, λ = 0.71073 Å, 69693 reflections collected, 11168 independent [R(int) = 0.050], which were used in calculations. R_1 = 0.0356, wR_2 = 0.0566 for observed unique reflections [$I > 2\sigma(I)$] and R_1 = 0.0659, wR_2 = 0.0745 for all unique reflections. Max. and min. residual electron densities 3.01 and -1.54 e Å⁻³. CCDC ref.: 1002301.

(5-Mes)(5-Mes')IrHCl (3). A solution of **2** (450 mg, 0.47 mmol) in toluene (40 mL) was heated to 70 °C for 48 h. Volatiles were removed in vacuo and the red residue extracted with diethyl ether (3 x 20 mL). Concentration and storage at -30 °C yielded bright red, X-ray quality crystals in 79% yield (310 mg). ¹H NMR (C₆D₆, 300 MHz, 298 K): δ_{H} 6.79 (4H, s, *meta*-CH Mes), 6.73 (1H, s, *meta*-CH Mes'), 6.70 (2H, s, *meta*-CH Mes'), 6.67 (1H, s, *meta*-CH Mes'), 3.52 (2H, br m, NCH₂), 3.18 (4H, s, NCH₂), 2.94 (2H, m, NCH₂), 2.42 (6H, s, *para*-CH₃ Mes), 2.41 (2H, br, IrCH₂), 2.33 (12H, s, *ortho*-CH₃ Mes), 2.18 (6H, s, *ortho*-CH₃ Mes), 1.91 (3H, s, *para*-CH₃ Mes'), 1.74 (3H, s, *ortho*-CH₃ Mes'), -32.84 (1H, s, IrH). ¹³C NMR (C₆D₆, 75 MHz, 298 K): δ_{C} 210.4, 209.9 (NCN), 137.9 (NC Mes'), 137.8 (NC Mes), 137.5 (NC Mes'), 137.0 (*para*-C Mes), 136.9, 136.4 (*para*-C Mes'), 136.1 (*ortho*-C Mes'), 135.8 (*ortho*-C Mes), 133.1 (*ortho*-C Mes'), 129.6, 129.5, 129.5 (*meta*-CH Mes'), 129.2 (*meta*-CH Mes'), 52.0, 51.3, 50.5, 49.4 (NCH₂), 21.3 (*para*-CH₃ Mes), 21.3, 21.2, 21.2 (*para*-CH₃ Mes'), 19.7, 19.4, 19.2 (*ortho*-CH₃ Mes'), 18.9 (*ortho*-CH₃ Mes). MS (EI +ve): m/z (%) 802.4 (1) [M-HCl]⁺. Elemental analysis (meas.): C 59.80, H 6.63, N 6.91. (calc.): C 60.02, H 6.23, N 6.66. Crystallography (for **3**): C₄₂H₅₂IrN₄Cl, M_r = 840.57, monoclinic, $P2_1/n$, a = 15.8693(1), b = 12.3445(1), c = 21.1450(2) Å, β = 104.697(1)°, V = 4006.8(1) Å³, Z = 4, ρ_c = 1.393 Mg m⁻³, T = 150 K, λ = 0.71073 Å, 138077 reflections collected, 9099 independent [R(int) = 0.024], which were used in calculations. R_1 = 0.0282, wR_2 = 0.0611 for observed unique reflections [$I > 2\sigma(I)$] and R_1 = 0.0424, wR_2 = 0.0732 for all unique reflections. Max. and min. residual electron densities 1.50 and -1.43 e Å⁻³. CCDC ref.: 1002302.

(6-Mes)₂IrH₃ (4). A solution of **1** (50 mg, 0.06 mmol) in toluene (10 mL) in a high pressure flask was freeze-pump-thaw degassed and back filled with dihydrogen to a pressure of ca. 4 atm. The reaction mixture was warmed to room temperature and stirred for 3 h, over which time a colour change was observed from orange to pale yellow. Conversion was judged to be quantitative by ¹H NMR spectroscopy when maintained under a H₂ atmosphere. ¹H NMR (C₆D₆, 300 MHz, 298 K): δ_{H} 6.90 (8H, s, *meta*-CH), 2.63 (8H, t, ³ J_{HH} = 5.4 Hz, NCH₂), 2.41 (12H, s, *para*-CH₃), 2.10 (24H, s, *ortho*-CH₃), 1.30 (4H, qn, ³ J_{HH} = 5.4 Hz, NCH₂CH₂), -9.75 (3H, s, IrH₃). ¹³C NMR (C₆D₆, 126 MHz, 298 K): δ_{C} 188.9 (NCN), 149.0 (NC Mes), 133.4 (*para*-C Mes), 132.9 (*ortho*-C Mes), 128.1 (*meta*-CH Mes), 44.3 (NCH₂), 20.9 (NCH₂CH₂), 20.0 (*para*-CH₃ Mes), 17.9

(*ortho*-CH₃ Mes). MS (CI^{-ve}): *m/z* (%) 836.4 (100) M⁺. Reproducible elemental microanalysis for **4** proved impossible to obtain due to the tendency of the compound to decompose other than when under a dihydrogen atmosphere. Single crystals of **4** suitable for X-ray crystallography were obtained from toluene solution under an overpressure of dihydrogen. However, the quality of the structure solution was poor and only sufficient to determine the heavy atom skeleton.

(5-*Mes*)₂IrH₂Cl (**5**). In a Young's ampoule, a solution of **3** (200 mg, 0.24 mmol) in toluene (15 mL) was freeze-pump-thaw degassed and back filled with dihydrogen to a pressure of ca. 4 atm. The reaction mixture was warmed to room temperature and stirred for 1 h, over which time a colour change was observed from red to yellow. Conversion was judged to be quantitative by ¹H NMR spectroscopy. X-ray quality crystals of **5** were isolated from a concentrated solution in diethyl ether stored at -30 °C. ¹H NMR (C₆D₆, 300 MHz, 298 K): δ_H 6.78 (s, 8H, *meta*-CH), 3.08 (s, 8H, NCH₂), 2.34 (s, 12H, *para*-CH₃), 2.19 (s, 24H, *ortho*-CH₃), -32.81 (s, 2H, IrH). ¹³C NMR (C₆D₆, 126 MHz, 298 K): δ_C 210.4 (NCN), 137.9 (NC Mes), 137.0 (*para*-C Mes), 135.8 (*ortho*-C Mes), 129.2 (*meta*-CH Mes), 50.5 (NCH₂), 21.3 (*para*-CH₃), 18.9 (*ortho*-CH₃). MS (EI +ve): *m/z* (%) 842.4 (5) M⁺. Accurate mass ([C₄₂H₅₄N₄¹⁹¹IrCl]⁺): 840.3639 (meas.), 840.3643 (calc.). Crystallography (for **5**): C₄₂H₅₄IrN₄Cl, *M_r* = 842.59, orthorhombic, *Pbca*, *a* = 17.0027(1), *b* = 19.4001(1), *c* = 23.4149(2) Å, *V* = 7723.50(9) Å³, *Z* = 8, ρ_c = 1.449 Mg m⁻³, *T* = 150 K, λ = 0.71073 Å, 158718 reflections collected, 8784 independent [R(int) = 0.033], which were used in calculations. *R*₁ = 0.0311, *wR*₂ = 0.0542 for observed unique reflections [*I* > 2σ(*I*)] and *R*₁ = 0.0643, *wR*₂ = 0.0768 for all unique reflections. Max. and min. residual electron densities 2.51 and -1.75 e Å⁻³. CCDC ref.: 1002303.

(6-*Mes*)(6-*Mes'*)IrHCl (**6**). A solution of HCl in diethyl ether (0.06 mL of a 2.0 M solution, 0.12 mmol) was added to a stirred solution of **1** (100 mg, 0.12 mmol) also in diethyl ether (20 mL). A colour change from orange to yellow was observed on addition. After 15 min, volatiles were removed in vacuo to give the yellow product which was isolated in 90% yield (93 mg) and >95% purity (by NMR) without further purification. ¹H NMR (C₆D₆, 300 MHz, 298 K): δ_H 7.04 (1H, s, *meta*-H Mes'), 6.92 (1H, s, *meta*-H Mes'), 6.83 (1H, s, *meta*-H Mes'), 6.74 (2H, s, *meta*-H Mes'), 6.65 (2H, s, *meta*-H Mes'), 6.64 (1H, s, *meta*-H Mes'), 3.33 (1H, d, ³*J*_{HH} = 10.9 Hz, NCH₂ Mes'), 2.97 (1H, m, NCH₂), 2.78 (2H, m, NCH₂), 2.73 (4H, m, NCH₂), 2.61 (3H, s, *para*-CH₃ Mes), 2.49 (6H, s, *para*-CH₃ Mes), 2.40 (3H, s, *para*-CH₃ Mes'), 2.36 (3H, s, *ortho*-CH₃ Mes), 2.30 (1H, d, ²*J*_{HH} = 11.5 Hz, IrCH₂), 2.25 (6H, s, *ortho*-CH₃ Mes), 2.19 (1H, d, ²*J*_{HH} = 11.5 Hz, IrCH₂), 2.18 (6H, s, *ortho*-CH₃ Mes), 1.87 (3H, s, *ortho*-CH₃ Mes'), 1.70 (3H, s, *ortho*-CH₃ Mes), 1.54 (2H, qn, ³*J*_{HH} = 5.7 Hz, NCH₂CH₂), 1.29 (1H, m, NCH₂CH₂), 1.15 (1H, m, NCH₂CH₂), -46.50 (1H, s, IrH). ¹³C NMR (C₆D₆, 75 MHz, 298 K): δ_C 207.4, 204.0 (both d, ²*J*_{CH} = 6.3 Hz, NCN), 144.1 (NC Mes'), 143.5, 143.4, 143.2 (NC Mes), 137.6, 135.9 (*para*-C Mes), 135.5 (*para*-C Mes'), 134.7, 134.5, 133.7, 133.6 (*ortho*-C Mes), 129.8 (*meta*-CH Mes'), 129.3, 129.2, 129.0, 128.4 (*meta*-CH Mes), 126.6 (*meta*-CH Mes'), 126.2 (*ortho*-C Mes'), 48.8, 48.3 (s, NCH₂), 47.3, 47.3 (NCH₂), 22.4, 21.7 (NCH₂CH₂), 21.3, 21.1, 20.8 (*para*-CH₃), 20.6 (*ortho*-CH₃ Mes'), 20.1, 19.6, 18.8, 16.8 (*ortho*-CH₃), -13.2 (d, ²*J*_{CH} = 10.1 Hz, IrCH₂). MS (EI +ve): *m/z* (%) 868.4 M⁺. Accurate mass ([C₄₄H₅₆N₄¹⁹¹IrCl]⁺): 866.3798 (meas.), 866.3799 (calc.).

(6-*Mes*)₂IrHCl₂ (**7**). A solution of HCl in diethyl ether (0.03 mL of a 2.0 M solution, 0.06 mmol) was added to a stirred solution of **1** (25 mg, 0.03 mmol) also in diethyl ether (10 mL). The solution was observed to turn from orange to yellow and back to orange in colour.

Stirring was allowed to continue for 10 min after which time the volatiles were removed in vacuo. The product was collected as a pale orange solid in 83% yield (22 mg) and >95% purity (by NMR) without further purification. ¹H NMR (C₆D₆, 300 MHz, 298 K): δ_H 6.79 (8H, s, *meta*-CH), 2.68 (8H, t, ³*J*_{HH} = 6 Hz, NCH₂), 2.35 (12H, s, *para*-CH₃), 2.27 (24H, s, *ortho*-CH₃), 1.40 (4H, qn, ³*J*_{HH} = 6 Hz, -49.80 (1H, s, IrH). ¹³C NMR (C₆D₆, 126 MHz, 298 K): δ_C 198.2 (d, ²*J*_{CH} = 6.7 Hz, NCN), 145.4 (NCMes), 136.8 (*para*-C Mes), 135.3 (*ortho*-C Mes), 130.3 (*meta*-CH Mes), 50.0 (NCH₂), 22.2 (NCH₂CH₂), 20.1 (*para*-CH₃ Mes), 19.6 (*ortho*-CH₃ Mes). MS (EI +ve): *m/z* (%) 830.3 (1) [M-2HCl]⁺, 904.3 (1) M⁺. Accurate mass ([C₄₄H₅₇N₄¹⁹¹Ir³⁵Cl₂]⁺): 902.3444 (meas.), 902.3566 (calc.).

(6-*Mes*)₂IrH₂Cl (**8**). A solution of **6** (50 mg, 0.06 mmol) in toluene (20 mL) in a high pressure flask was freeze-pump-thaw degassed and back filled with dihydrogen to a pressure of ca. 4 atm. The reaction mixture was warmed to room temperature and stirred for 3 h. Removal of volatiles in vacuo yielded the yellow solid product in 84% yield (44 mg). Yellow crystals suitable for X-ray crystallography were obtained from a concentrated solution in diethyl ether at 20 °C. ¹H NMR (C₆D₆, 300 MHz, 298 K): δ_H 6.81 (8H, s, *meta*-CH), 2.57 (8H, t, ³*J*_{HH} = 6.0 Hz, NCH₂), 2.36 (12H, s, *para*-CH₃), 2.15 (24H, s, *ortho*-CH₃), 1.37 (4H, qn, ³*J*_{HH} = 6.0 Hz, NCH₂CH₂) -33.05 (2H, s, IrH₂). ¹³C NMR (C₆D₆, 126 MHz, 298 K): δ_C 205.1 (NCN), 145.7 (NC Mes), 136.3 (*para*-C Mes), 135.1 (*ortho*-C Mes), 130.6 (*meta*-CH Mes), 48.6 (NCH₂), 22.8 (NCH₂CH₂), 22.0 (*para*-CH₃ Mes), 19.9 (*ortho*-CH₃ Mes). MS (EI +ve): *m/z* (%) 830.4 (1) [M-Cl]⁺. Elemental analysis (meas.): C 60.88, H 6.60, N 7.06. (calc.): C 60.70, H 6.71, N 6.44. Crystallography (for **8**): C₄₄H₅₆IrN₄Cl, *M_r* = 868.63, orthorhombic, *F* dd2, *a* = 42.9414(5), *b* = 21.5369(3), *c* = 8.42331(9) Å, *V* = 7790.10(15) Å³, *Z* = 8, ρ_c = 1.481 Mg m⁻³, *T* = 150 K, λ = 1.54180 Å, 21447 reflections collected, 2192 independent [R(int) = 0.029], which were used in calculations. *R*₁ = 0.0211, *wR*₂ = 0.0571 for observed unique reflections [*I* > 2σ(*I*)] and *R*₁ = 0.0211, *wR*₂ = 0.0571 for all unique reflections. Max. and min. residual electron densities 1.06 and -1.01 e Å⁻³. CCDC ref.: 1002304.

[(6-*Xyl*)₂IrH₂][BAR^{*f*}₄] (**9**). A solution of [(6-*Xyl*)(6-*Xyl'*)IrH][BAR^{*f*}₄] (40 mg, 0.02 mmol) prepared in situ from **1**' and [H(OEt)₂][BAR^{*f*}₄] in fluorobenzene (10 mL) was freeze-pump-thaw degassed and backfilled with dihydrogen gas to ca. 4 atm. The reaction mixture was stirred over 1 h, during which time the solution turned from orange to yellow. The volatiles were removed in vacuo and the remaining yellow solid was washed with hexanes (2 x 10 mL) and dried in vacuo (yield 52%, 17 mg). Crystals suitable for X-ray crystallography were obtained by layering a fluorobenzene solution with pentane and storage at 20 °C. ¹H NMR (CD₂Cl₂, 300 MHz, 298 K): δ_H 7.72 (s, 8H, *ortho*-CH [BAR^{*f*}₄]), 7.55 (s, 4H, *para*-CH [BAR^{*f*}₄]), 7.24 (tr, ³*J*_{HH} = 7.4 Hz, 4H, *para*-CH), 7.15 (d, ³*J*_{HH} = 7.5 Hz, 8H, *meta*-CH), 3.14 (tr, ³*J*_{HH} = 5.7 Hz, 8H, NCH₂), 2.11 (qn, ³*J*_{HH} = 5.7 Hz, 4H, NCH₂CH₂), 1.83 (s, 24H, *ortho*-CH₃), -43.82 (s, 2H, IrH). ¹³C NMR (CD₂Cl₂, 125 MHz, 298 K): δ_C 200.6 (NCN), 162.3 (q, ¹*J*_{CB} = 49.3 Hz, CB [BAR^{*f*}₄]), 138.7 (NC Xyl), 137.0 (*ortho*-C Xyl), 135.4 (br, *ortho*-CH [BAR^{*f*}₄]), 129.8 (*para*-CH Xyl), 129.5 (*meta*-CH Xyl), 129.3 (m, *meta*-C [BAR^{*f*}₄]), 125.2 (q, ¹*J*_{CF} = 271.0 Hz, CF₃ [BAR^{*f*}₄]), 118.0 (m, *para*-CH [BAR^{*f*}₄]), 46.6 (NCH₂), 21.3 (NCH₂CH₂), 18.4 (*ortho*-CH₃). Elemental analysis (meas.): C 49.76; H 3.44; N 3.44. (calc.): C 49.90; H 3.66; N 3.64. Crystallography (for **9**): C₆₄H₅₆BF₂₄IrN₄, *M_r* = 1642.29, monoclinic, *P* 2₁/n, *a* = 22.1025(2), *b* = 14.5368(1), *c* = 23.3691(2) Å, β = 111.973(1)°, *V* = 6963.1(1) Å³, *Z* = 4, ρ_c = 1.567 Mg m⁻³, *T* = 150 K, λ = 0.71073 Å, 88057 reflections collected, 15868 independent [R(int) = 0.055], which were used in calculations. *R*₁ = 0.0476, *wR*₂

$= 0.0777$ for observed unique reflections [$I > 2\sigma(I)$] and $R_1 = 0.0879$, $wR_2 = 0.1074$ for all unique reflections. Max. and min. residual electron densities 2.84 and $-2.84 \text{ e } \text{\AA}^{-3}$. CCDC ref.: 1002305.

Preparation of [(5-Mes)₂IrH₂(κ²-H₃BNMe₃)] [BAR₄^f] (10). A solution of Na[BAR₄^f] (53 mg, 0.06 mmol) in THF (10 mL) was added at -30°C to a stirred solution containing **5** (50 mg, 0.06 mmol) and H₃BNMe₃ (43 mg, 0.6 mmol) also in THF (20 mL). The reaction mixture was stirred whilst warming to room temperature over 1 h, during which time the yellow colour paled. Precipitated solid was removed by filtration and the volatiles were removed in vacuo. The remaining pale yellow solid was washed with hexanes (3 x 10 mL) and dried in vacuo (yield 52%, 54 mg). Crystals suitable for X-ray crystallography were obtained by layering a fluorobenzene solution with pentane and storage at 20°C . ¹H NMR (CD₂Cl₂, 300 MHz, 298 K): δ_H 7.73 (s, 8H, *ortho*-CH [BAR₄^f]), 7.57 (s, 4H, *para*-CH [BAR₄^f]), 6.80 (s, 8H, *meta*-CH), 3.67 (s, 8H, NCH₂), 2.36 (s, 24H, *ortho*-CH₃), 2.24 (s, 12H, *para*-CH₃), 1.93 (s, br, 9H, NMe₃), -2.11 (br s, 3H, BH₃), -21.86 (s, 2H, IrH). ¹³C NMR (CD₂Cl₂, 75 MHz, 298 K): δ_C 198.8 (NCN), 162.1 (qt, ¹J_{CB} = 49.6 Hz, CB [BAR₄^f]), 137.9 (NC Mes), 137.7 (*para*-C Mes), (*ortho*-C Mes), 135.1 (br, *ortho*-CH [BAR₄^f]), 129.8 (*meta*-CH Mes), 129.2 (m, *meta*-C [BAR₄^f]), 124.9 (qt, ¹J_{CF} = 271.0 Hz, CF₃ [BAR₄^f]), 117.8 (m, *para*-CH [BAR₄^f]), 52.7 (NCH₂), 51.4 (NMe₃), 46.1, 21.1 (*para*-CH₃ Mes), 18.9 (*ortho*-CH₃ Mes). ¹¹B NMR (CD₂Cl₂, 96 MHz, 298 K): δ_B 13.0 (s, BH₃), -6.9 (s, [BAR₄^f]). ¹⁹F NMR (CD₂Cl₂, 282 MHz, 298 K): δ -62.87 (s, [BAR₄^f]). MS (EI +ve): *m/z* (%) 807.4 (6) [M-H₃BNMe₃]⁺, 880.5 (4) M⁺. Accurate mass ([C₄₅H₆₆N₅¹¹B¹⁹¹Ir]⁺): 880.5180 (meas.), 880.5045 (calc.). Crystallography (for **10**): C₇₇H₇₈IrN₅B₂F₂₄, M_r = 1743.29, triclinic, *P*-1, a = 12.5841(2), b = 17.9389(3), c = 18.2196(3) Å, α = 86.8231(6), β = 69.9280(7), γ = 87.6703(6)°, V = 3856.21(11) Å³, Z = 2, ρ_c = 1.501 Mg m⁻³, T = 150 K, λ = 0.71073 Å, 60623 reflections collected, 17332 independent [R(int) = 0.070], which were used in calculations. R₁ = 0.0552, wR₂ = 0.0877 for observed unique reflections [$I > 2\sigma(I)$] and R₁ = 0.1004, wR₂ = 0.1205 for all unique reflections. Max. and min. residual electron densities 6.73 and $-4.41 \text{ e } \text{\AA}^{-3}$. CCDC ref.: 1002306.

Preparation of [(5-Mes)₂IrH₂(κ²-H₃BNHMe₂)] [BAR₄^f] (11) and [(5-Mes)₂IrH₂(κ²-H₂BNMe₂)] [BAR₄^f] (12). A solution of Na[BAR₄^f] (53 mg, 0.06 mmol) in THF (10 mL) was added at -78°C to a stirred solution containing **5** (50 mg, 0.06 mmol) and H₃BNHMe₂ (35 mg, 0.6 mmol) also in THF (10 mL). The reaction mixture was stirred whilst warming to room temperature over 1 h, during which time the yellow colour paled. The solution was filtered and volatiles removed in vacuo. The residue was washed with hexanes (2 x 10 mL), dried under vacuum and collected a pale yellow powder in 59% yield (61 mg). Crystals suitable for X-ray and neutron diffraction studies were obtained from a fluorobenzene solution layered with pentane and stored at 20°C . These were shown by a combination of diffraction techniques to be a 4:6 mixture of **11** and **12**. On re-dissolution of single crystalline samples in deuterated solvent for NMR measurements further dehydrogenation of **11** occurs, yielding solutions in which **12** is the overwhelmingly major constituent (ca. 90%). ¹H NMR (CD₂Cl₂, 300 MHz, 298 K): δ_H 7.72 (s, 8H, *ortho*-CH [BAR₄^f]), 7.56 (s, 4H, *para*-CH [BAR₄^f]); (i) signals corresponding to the major component (H₂BNMe₂ complex **12**): 6.84 (s, 8H, *meta*-CH Mes), 3.74 (s, 8H, NCH₂), 2.46 (s, 6H, NMe₂), 2.36 (s, 12H, *para*-CH₃ Mes), 1.87 (s, 24H, *ortho*-CH₃ Mes), -6.18 (br, 2H, BH₂), -15.70 (d, ²J_{HH} = 13.5 Hz, 2H, IrH); (ii) distinct signals corresponding to the minor component (H₃BNHMe₂ complex **11**): 6.88 (s, 8H, *meta*-CH Mes), 3.78 (s, 8H, NCH₂), 2.46 (s, 6H, NMe₂), 2.33 (s, 12H, *para*-CH₃ Mes), 1.90 (s, 24H, *ortho*-CH₃ Mes), -20.51 (s, 2H, IrH). ¹³C NMR (CD₂Cl₂, 75 MHz, 298 K):

δ_C 187.5 (NCN), 162.1 (qt, ¹J_{CB} = 49.6 Hz, CB [BAR₄^f]), 138.4 (NC Mes), 137.4 (*para*-C Mes), 135.9 (*ortho*-C Mes), 135.2 (br, *ortho*-CH [BAR₄^f]), 129.9 (*meta*-CH Mes), 129.2 (*meta*-C [BAR₄^f]), 124.9 (qt, ¹J_{CF} = 271.0 Hz, CF₃ [BAR₄^f]), 117.8 (m, *para*-CH [BAR₄^f]), 50.5 (NCH₂), 41.1 (NCH₃), 21.2 (*para*-CH₃ Mes), 17.8 (*ortho*-CH₃ Mes). ¹¹B NMR (CD₂Cl₂, 96 MHz, 298 K): δ_B 48.1 (br, BH₂), 10.8 (s, BH₃), -6.9 (s, [BAR₄^f]). ¹⁹F NMR (CD₂Cl₂, 282 MHz, 298 K): δ -62.89 (s, [BAR₄^f]). MS (ESI +ve): *m/z* 864.5 (100) M⁺. Accurate mass ([C₄₄H₆₂N₅¹¹B¹⁹²Ir]⁺): 864.4834 (meas.), 864.4732 (calc.). Elemental analysis (meas.): C 52.73, H 4.76, N 3.68. (calc. for a 4:6 co-crystallite of **11** and **12**): C 52.81, H 4.36, N 4.05. X-ray crystallography (43:57 co-crystal of **11** and **12**): C₇₆H_{74.86}B₂F₂₄IrN₅, M_r = 1728.11, triclinic, *P*-1, a = 12.7291(1), b = 17.5467(2), c = 18.0256(2) Å, α = 88.273(1), β = 70.202(1), γ = 87.531(1)°, V = 3784.1(1) Å³, Z = 2, ρ_c = 1.517 Mg m⁻³, T = 100 K, λ = 0.71073 Å, 66843 reflections collected, 17236 independent [R(int) = 0.027], which were used in calculations. R₁ = 0.0411, wR₂ = 0.0947 for observed unique reflections [$I > 2\sigma(I)$] and R₁ = 0.0486, wR₂ = 0.1042 for all unique reflections. Max. and min. residual electron densities 2.80 and $-1.22 \text{ e } \text{\AA}^{-3}$. CCDC ref.: 1002307. Neutron Diffraction (35:65 co-crystal of **11** and **12**): C₇₆H_{74.86}B₂F₂₄IrN₅, M_r = 1728.11, triclinic, *P*-1, a = 12.689(3), b = 17.5549(16), c = 17.948(4) Å, α = 88.275(19), β = 70.175(17), γ = 87.82(2)°, V = 3757.7(14) Å³, Z = 2, ρ_c = 1.527 Mg m⁻³, T = 100 K, λ = Laue, 7639 independent reflections, which were used in calculations. R₁ = 0.0937, wR₂ = 0.2053 for observed unique reflections [$I > 2\sigma(I)$] and R₁ = 0.1060, wR₂ = 0.2162 for all unique reflections. Max. and min. residual electron densities $\sim 12\%$ of a carbon atom. CCDC ref.: 1002308.

Acknowledgements

EPSRC (studentships for NP, MJK, and access to the NMSF, Swansea University); NSERC (post-doctoral fellowship for JIB). Experiments at the ISIS Pulsed Neutron and Muon Source were supported by a beam-time allocation from the Science and Technology Facilities Council (RB1120229).

Notes and references

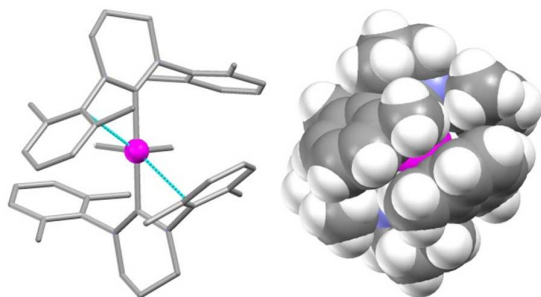
^a Inorganic Chemistry Laboratory, Department of Chemistry, University of Oxford, South Parks Road, Oxford, OX1 3QR, UK. E-mail: Simon Aldridge@chem.ox.ac.uk. ^b ISIS Facility, Rutherford Appleton Laboratory-STFC, Chilton, Didcot, Oxford OX11 0QX, UK.

† Electronic Supplementary Information (ESI) available: crystallographic data for all X-ray and neutron diffraction studies (as CIFs) – CCDC references 1002300-1002308. See DOI: 10.1039/b000000x/

- See, for example: (a) A. J. Arduengo, *Acc. Chem. Res.*, 1999, **32**, 913; (b) D. Bourissou, O. Guerret, F. P. Gabbaï and G. Bertrand, *Chem. Rev.*, 2000, **100**, 39; (c) F. E. Hahn and M. C. Jahnke, *Angew. Chem., Int. Ed.*, 2008, **47**, 3122; (d) T. Dröge and F. Glorius, *Angew. Chem., Int. Ed.*, 2010, **49**, 6940; (e) D. Martin, M. Melaimi, M. Soleilhavoup and G. Bertrand, *Organometallics*, 2011, **30**, 5304.
- See, for example: (a) W. A. Herrmann, *Angew. Chem., Int. Ed.*, 2002, **41**, 1290; (b) S. Würtz and F. Glorius, *Acc. Chem. Res.*, 2008, **41**, 1523; (c) R. Corberán, E. Mas-Márza and E. Peris, *Eur. J. Inorg. Chem.*, 2009, 1700; (d) J. C. Y. Lin, R. T. W. Huang, C. S. Lee, A. Bhattacharyya, W. S. Hwang and I. J. B. Lin, *Chem. Rev.*, 2009, **109**, 3561; (e) S. Díez-González, N. Marion and S. P. Nolan, *Chem. Rev.*, 2009, **109**, 3612.
- (a) M. Iglesias, D. J. Beetstra, J. C. Knight, L. L. Ooi, A. Stasch, S. Coles, L. Male, M. B. Hursthouse, K. J. Cavell, A. Dervisi and I. A. Fallis, *Organometallics*, 2008, **27**, 3279; (b) E. L. Kolychev, I. A. Portnyagin, V. V. Shuntikov, V. N. Khurstalev and M. S. Nechaev, *J. Organomet. Chem.*, 2009, **694**, 2454; (c) M. Iglesias, D. J. Beetstra, B. Kariuki, K. J. Cavell, A. Dervisi and I. A. Fallis, *Eur. J. Inorg.*

- Chem.* 2009, 1913; (d) S. Flügge, A. Anoop, R. Goddard, W. Thiel and A. Fürstner, *Chem.-Eur. J.*, 2009, **15**, 8558; (e) W. Y. Lu, K. J. Cavell, J. S. Wixey and B. Kariuki, *Organometallics*, 2011, **30**, 5649; (f) J. J. Dunsford, K. J. Cavell and B. Kariuki, *Organometallics*, 2012, **31**, 4118.
4. % V_{bur} : (a) A. C. Hillier, W. J. Sommer, B. S. Yong, J. L. Petersen, L. Cavallo and S. P. Nolan, *Organometallics*, 2003, **22**, 4322; (b) L. Cavallo, A. Correa, C. Costabile and H. Jacobsen, *J. Organomet. Chem.*, 2005, **690**, 5407; (c) A. Poater, B. Cosenza, A. Correa, S. Giudice, F. Ragone, V. Scarano and L. Cavallo, *Eur. J. Inorg. Chem.*, 2009, 1759; (d) S. Wurtz and F. Glorius, *Acc. Chem. Res.*, 2008, **41**, 1523; (e) F. Ragone, A. Poater and L. Cavallo, *J. Am. Chem. Soc.*, 2010, **132**, 4249; (f) H. Clavier and S. P. Nolan, *Chem. Commun.*, 2010, **46**, 841.
5. W. A. Herrmann, S. K. Schneider, K. Öfele, M. Sakamoto and E. Herdtweck, *J. Organomet. Chem.*, 2004, **689**, 2441.
6. (a) C. Y. Tang, W. Smith, D. Vidovic, A. L. Thompson, A. B. Chaplin and S. Aldridge, *Organometallics*, 2009, **28**, 3059; (b) C. Y. Tang, A. L. Thompson and S. Aldridge, *Angew. Chem., Int. Ed.*, 2010, **49**, 921; (c) C. Y. Tang, A. L. Thompson and S. Aldridge, *J. Am. Chem. Soc.*, 2010, **132**, 10578; (d) C. Y. Tang, J. Lednik, D. Vidovic, A. L. Thompson and S. Aldridge, *Chem. Commun.*, 2011, **47**, 2523; (e) C. Y. Tang, W. Smith, A. L. Thompson, D. Vidovic, S. Aldridge, *Angew. Chem., Int. Ed.*, 2011, **50**, 1359; (f) C. Y. Tang, N. Phillips, J. I. Bates, A. L. Thompson, M. J. Gutman and S. Aldridge, *Chem. Commun.*, 2012, **48**, 8096; (g) C. Y. Tang, N. Phillips, M. J. Kelly and S. Aldridge, *Chem. Commun.*, 2012, **48**, 11999; (h) N. Phillips, J. Rowles, M. J. Kelly, I. Riddlestone, N. H. Rees, A. Dervisi, I. A. Fallis and S. Aldridge, *Organometallics*, 2012, **31**, 8075; (i) N. Phillips, R. Tirfoin and S. Aldridge, *Chem.-Eur. J.*, 2014, **20**, 3825.
7. J. Huang, E. D. Stevens and S. P. Nolan, *Organometallics*, 2000, **19**, 1194.
8. For related iridium systems featuring a very high field ^1H NMR signal assigned to a hydride ligand *trans* to a vacant coordination site see, for example: (a) A. C. Cooper, W. E. Streib, O. Eisenstein and K. G. Caulton, *J. Am. Chem. Soc.*, 1997, **119**, 9069; (b) N. M. Scott, R. Dorta, E. D. Stevens, A. Correa, L. Cavallo and S. P. Nolan, *J. Am. Chem. Soc.*, 2005, **127**, 3516;
9. See, for example: W. J. Oldham, A. S. Hinkle and D. M. Heinekey, *J. Am. Chem. Soc.*, 1997, **117**, 11028.
10. (a) H. V. Nanishankar, S. Dutta, M. Nethaji and B. R. Jagirdar, *Inorg. Chem.*, 2005, **44**, 6203. See also: (b) M. Findlater, K. M. Schultz, W. H. Bernskoetter, A. Cartwright-Sykes, D. M. Heinekey and M. Brookhart, *Inorg. Chem.*, 2012, **51**, 4672.
11. G. J. Kubas in *Metal Dihydrogen and σ -Bond Complexes: Structure, Theory and Reactivity* Kluwer Academic/Plenum Publishers, New York, 2001.
12. J.-F. Riehl, Y. Jean, O. Eisenstein and M. Pélissier, *Organometallics*, 1992, **11**, 729.
13. See, for example: M. Findlater, W. H. Bernskoetter and M. Brookhart, *J. Am. Chem. Soc.*, 2010, **132**, 4534.
14. An alternative interpretation of **8** based on a trigonal bipyramidal geometry would be in line with the quantum chemical predictions of Eisenstein and co-workers: see reference 12.
15. J. Emsley, *The Elements* OUP, Oxford, 1997.
16. For recent reviews see, for example: (a) T. J. Clark, K. Lee, and I. Manners, *Chem.-Eur. J.*, 2006, **12**, 8634; (b) T. B. Marder, *Angew. Chem., Int. Ed.*, 2007, **46**, 8116; (c) F. H. Stephens, V. Pons, and R. T. Baker, *Dalton Trans.*, 2007, **2**, 2613; (d) C. W. Hamilton, R. T. Baker, A. Staubitz, and I. Manners, *Chem. Soc. Rev.*, 2009, **38**, 279; (e) N. C. Smythe and J. C. Gordon, *Eur. J. Inorg. Chem.*, 2010, 509; (f) A. Staubitz, A. P. M. Robertson, M. E. Sloan, and I. Manners, *Chem. Rev.*, 2010, **110**, 4023; (g) A. Staubitz, A. P. M. Robertson, and I. Manners, *Chem. Rev.*, 2010, **110**, 4079; (h) G. Alcaraz and S. Sabo-Etienne, *Angew. Chem., Int. Ed.*, 2010, **49**, 7170.
17. For other examples of κ^2 -coordinated aminoboranes, see: (a) G. Alcaraz, L. Vendier, E. Clot and S. Sabo-Etienne, *Angew. Chem., Int. Ed.*, 2010, **49**, 918; (b) G. Alcaraz, A. B. Chaplin, C. J. Stevens, E. Clot, L. Vendier, A. S. Weller and S. Sabo-Etienne, *Organometallics*, 2010, **29**, 5591; (c) C. J. Stevens, R. Dallanegra, A. B. Chaplin, A. S. Weller, S. A. Macgregor, B. Ward, D. McKay, G. Alcaraz and S. Sabo-Etienne, *Chem.-Eur. J.*, 2011, **17**, 3011. For related κ^1 systems, see: (d) D. Vidovic, D. A. Addy, T. Krämer, J. McGrady and S. Aldridge, *J. Am. Chem. Soc.*, 2011, **133**, 8494.
18. T. M. Douglas, A. B. Chaplin, A. S. Weller, X. Yang and M. B. Hall, *J. Am. Chem. Soc.*, 2009, **131**, 15440.
19. T. M. Trnka, J. P. Morgan, M. S. Sandford, T. E. Wilhelm, M. Scholl, T.-L. Choi, S. Ding, M. W. Day and R. H. Grubbs, *J. Am. Chem. Soc.*, 2003, **125**, 2546.
20. J. L. Herde, J. C. Lambert and C. V. Senoff, *Inorg. Synth.*, 1974, **15**, 18.
21. D. L. Reger, T. D. Wright, C. A. Little, J. J. S. Lamba and M. D. Smith, *Inorg. Chem.*, 2001, **40**, 3810.
22. M. Brookhart, B. Grant and A. F. Volpe, Jr., *Organometallics*, 1992, **11**, 3920.
23. S. R. Bahr and P. Boudjouk, *J. Org. Chem.*, 1992, **57**, 5545.
24. (a) Z. Otwinowski and W. Minor, *Processing of X-Ray Diffraction Data Collected in Oscillation Mode, Methods Enzymol.*, Sweet Academic Press, 1997; (b) A. Altomare, G. Casciaro, C. Giacovazzo, A. Guagliardi, M. C. Burla, G. Polidori and M. Camalli, *J. Appl. Crystallogr.* 1994, **27**, 435; (c) L. Palatinus and G. Chapuis, *J. Appl. Crystallogr.*, 2007, **40**, 786; (d) R. I. Cooper, A. L. Thompson and D. J. Watkin, *J. Appl. Crystallogr.*, 2010, **43**, 1100; (e) A. L. Thompson and D. J. Watkin, *J. Appl. Crystallogr.*, 2011, **44**, 1017.
25. (a) H. D. Flack, *Acta Crystallogr.*, 1983, **A39**, 876; (b) H. D. Flack and G. Bernardinelli, *J. Appl. Crystallogr.* 2000, **33**, 1143.
26. R. I. Cooper, R. O. Gould, S. Parsons and D. J. Watkin, *J. Appl. Crystallogr.*, 2002, **35**, 168.
27. (a) A. Spek, *J. Appl. Crystallogr.*, 2003, **36**, 7; (b) P. van der Sluis and A. L. Spek, *Acta Crystallogr.*, 1990, **A46**, 194.
28. D. A. Keen, M. J. Gutmann and C. C. Wilson, *J. Appl. Cryst.*, 2006, **39**, 714.
29. G. M. Sheldrick, *Acta Cryst.*, 2008, **A64**, 112.

For Table of Contents



Critical influence of NHC ring size: highly labile $[\text{Ir}(\text{5-Mes})_2(\text{H})_2]^+$ can only be studied by trapping experiments, while $[\text{Ir}(\text{6-Mes})_2(\text{H})_2]^+$ and $[\text{Ir}(\text{6-Xyl})_2(\text{H})_2]^+$ are air/moisture stable,